Voltage control of the spin-dependent interaction constants of dipolaritons and its application to optical parametric oscillators

A. V. Nalitov,[1] D. D. Solnyshkov,[1] N. A. Gippius,[2,3] and G. Malpuech[1]

[1]*Institut Pascal, PHOTON-N2, Clermont Université, Blaise Pascal University, CNRS, 24 Avenue des Landais, 63177 Aubière Cedex, France*

[2]*Skolkovo Institute of Science and Technology, 100 Novaya St., Skolkovo, Odintsovsky District, Moscow Region 143025, Russia*

[3]*A. M. Prokhorov General Physics Institute, RAS, Vsavilova Street 38, Moscow 119991, Russia*

(Received 10 October 2014; revised manuscript received 5 November 2014; published 1 December 2014)

A dipolariton is a voltage-controlled mixture of direct and indirect excitons in asymmetric double quantum wells coupled by resonant carrier tunneling, and a microcavity photon. We calculate the voltage dependence of the spin-singlet and spin-triplet interaction parameters α_1 and α_2. Both parameters can reach values 1 order of magnitude larger than that of exciton-polaritons thanks to the strong interaction between indirect excitons. We show that the variation of the indirect exciton fraction of the dipolaritons induces a change of sign of α_2: the interaction passes from attractive to repulsive with increasing voltage. For large enough voltage, α_2 becomes larger than α_1, which in principle can lead to the formation of a circularly polarized dipolariton condensate. We propose an application of the α_2 dependence to a voltage-controlled dipolaritonic optical parametric oscillator. The change of sign of α_2 allows on-site control of the linear polarization degree of the optical signal and its on-demand inversion.

DOI: 10.1103/PhysRevB.90.235304 PACS number(s): 71.36.+c, 42.65.Yj

I. INTRODUCTION

Cavity exciton-polaritons are mixed exciton-photon quasiparticles formed by the strong coupling between cavity photons and quantum well excitons [1]. They interact strongly between each other because of their excitonic component. They represent one of the best examples of interacting photons implementing the concept of photonic quantum fluid [2]. From an applied point of view, these strongly interacting photonic particles represent a unique opportunity for the realization of low-threshold nonlinear optical devices [3–8]. The typical way to modify the strength of the polariton-polariton interaction is to change the excitonic content of the polariton by changing the energy detuning between the bare exciton and photon energy [9]. Using this approach, changing the interaction constants means changing the position of the experiment on a wedged sample. Polaritons are also spinor particles with a spin structure similar to that of photons [10]. Their interactions are strongly spin anisotropic. Indeed, quantum well Wannier $1s$ excitons do not possess a dipole moment, and the main mechanism of their interaction in the case of small transferred momentum is the short-range exchange interaction [11]. We will call the interaction parameter in the triplet configuration (same spins) α_1. If one considers two polaritons with opposite spins, the exchange of the carriers of their excitonic part leads to the formation of dark excitonic states of total angular momentum ± 2, whose separation from the polariton states is of the order of the Rabi splitting. An alternative mechanism of interaction between dipolaritons having opposite spins is associated with the formation of an intermediate biexciton state [12–14]. As a result, interaction between polaritons of opposite spins described by an interaction parameter α_2 is a second-order process. One should notice that far from the biexciton resonance it is strongly suppressed compared to the first-order carrier exchange interaction α_1 and is weakly attractive. This fact had numerous consequences, verified by multiple experiments, such as the linear polarization of polariton condensates [15–17], structure of topological defects [18,19], polarization inversion in polariton optical parametric oscillators [20], multistability effects [5,21], and others. On the other hand, when the polariton state is approaching the biexciton energy, α_2 increases and it can even change sign while crossing the resonance [13,14]. This interesting mechanism of control of the sign of the interaction parameter is, however, necessarily associated with strong losses in the resonant biexciton state, and also by a large thermal depletion of the polariton states [5,22].

If we now consider the indirect excitons (IXs) in coupled quantum wells (CQWs), they are formed by an electron and a heavy hole in neighboring CQWs and thus have a dipole moment oriented along the growth direction (due to the applied bias) and proportional to the CQW separation distance d. Consequently, the dipole-dipole repulsion of IXs is a first-order effect and is even stronger than their exchange interaction, which switches from repulsive to attractive while increasing d [23,24]. However, the coupling of an IX with a cavity photon mode is limited by the small oscillator strength of the IX, proportional to the overlap of the vanishing tails of the electron and hole wave functions in the barriers.

Recently, exploiting the asymmetric double quantum wells (ASDQWs) for resonant tunnel coupling of IX to the conventional direct exciton (DX), their bound state was suggested and realized [25]. The ASDQW embedded in a microcavity structure is schematically shown on Fig. 1. The coupling of three modes, indirect and direct exciton and cavity photon, gives rise to a new two-dimensional quasiparticle - *dipolariton*. Being thus a mixture of dipolar matter and light, dipolaritons represent photons with strong dipolar interaction.

In this work we theoretically describe the voltage dependence of the spin anisotropic interaction between dipolaritons and see how this dependence can be exploited in a practical application. We demonstrate that the interaction of dipolaritons is at least 1 order of magnitude stronger than that of conventional polaritons. We also show that the nature of the interaction between dipolaritons of opposite spins can

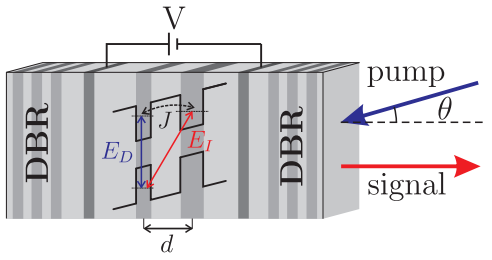

FIG. 1. (Color online) A sketch of the studied system. The asymmetric double quantum well (ASDQW) is situated between the contacts and two Bragg reflectors forming a microcavity. Voltage V, applied to the contacts, shifts the energy diagram of the ASDQW and the energies of the indirect ($E_{\rm IX}$) and direct ($E_{\rm DX}$) exciton states, coupled via tunneling of the electron through the barrier.

be switched from attractive to repulsive. We illustrate this dependence by calculating the polarization response of a dipolaritonic optical parametric oscillator (DOPO). This effect manifests itself in the linear polarization inversion of the DOPO that can be switched by an applied voltage. We also predict bistable behavior of the DOPO emission versus the pumping intensity and the applied voltage.

The present work is organized as follows. The spin-dependent dipolariton wave functions are calculated in Sec. II. The calculation of the matrix elements of the interaction between dipolaritons is described in Sec. III. The analysis of the suggested dipolaritonic OPO scheme is given in Sec. IV. Discussion of the obtained results concludes the work in Sec. V.

II. GENERAL DESCRIPTION, CALCULATION OF THE DIPOLARITON WAVE FUNCTIONS

We consider a structure consisting of ASDQWs embedded in a microcavity composed of two Bragg mirrors (Fig. 1). The DX state is formed by an electron-hole pair in the ground state, confined in one QW, while the IX consists of a hole in the same QW as that of the DX and an electron in the other QW. The DX and IX are thus coupled via the electron tunneling through the barrier, described by the coupling constant J, while the DX coupling to the cavity mode is induced by the exciton oscillator strength, giving rise to the Rabi splitting Ω.

The ASDQWs are subject to an external electric field, normal to their plane, produced by a voltage V, applied to the contacts on the doped layers [26]. The field shifts electron and hole levels of size quantization in both QWs, so that the DX energy $E_{\rm DX}(V) = E_{\rm DX}(0) - \beta V^2$ slowly decreases, depending quadratically on the field, due to the quantum confined Stark effect [27]. On the other hand, the IX energy $E_{\rm IX}(V) = E_{\rm IX}(0) - \gamma V$ shift is steeper and depends linearly on the field with the proportionality coefficient being the IX dipole moment [28]. In the absence of field, $E_{\rm IX}(0) > E_{\rm DX}(0)$. Therefore, at a certain voltage V_0 both exciton states have the same energy and become resonantly coupled. We consider the range of voltages around V_0, where the IX energy shift is smaller than the energy distance to the nearest electron confinement level or the closest cavity photon mode. This allows us to neglect the presence of other states and to write the following system Hamiltonian [25]:

$$H(Q,V) = \begin{pmatrix} E_{\rm IX}(V) & -J/2 & 0 \\ -J/2 & E_{\rm DX}(V) & -\Omega/2 \\ 0 & -\Omega/2 & E_{\rm C} + T_{\rm C}(Q) \end{pmatrix}, \quad (1)$$

where the term $T_{\rm C}(Q) = \hbar^2 Q^2/2m_{\rm C}$ accounts for the propagation of light in the cavity plane and represents the kinetic energy of the confined photon. Here $\mathbf{Q}$ is the wave vector in the cavity plane and $m_{\rm C}$ stands for the effective mass of the cavity photon. Similar terms for excitons may be safely neglected due to the large exciton mass $m_{\rm I} = m_{\rm D} \sim 10^4 m_{\rm C}$.

Diagonalization of the Hamiltonian (1) gives three dipolariton branches resulting from the strong coupling between the three initial resonances. They are shown as a function of voltage V on Fig. 2(a), while Fig. 2(b) demonstrates the dispersion of the branches for a given applied bias. The

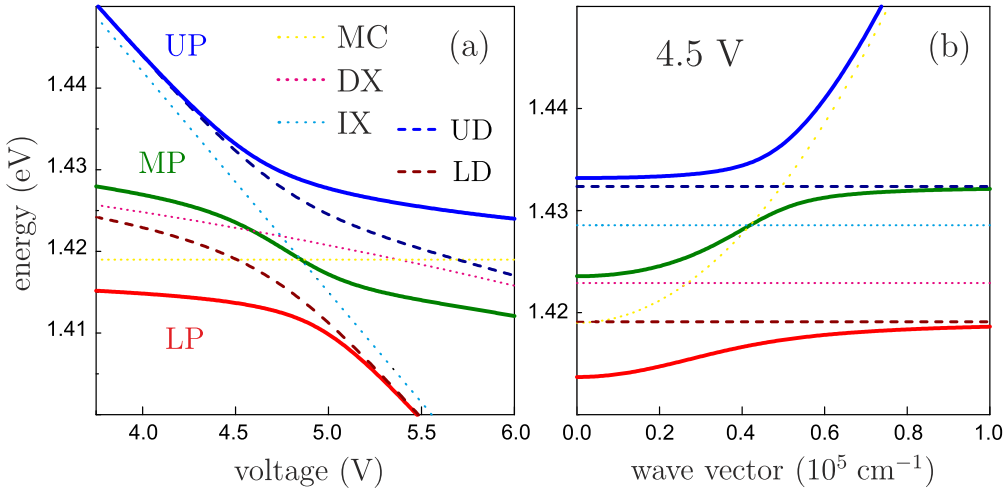

FIG. 2. (Color online) Dipolaritonic branches stemming from direct (DX) and indirect (IX) excitonic and microcavity photonic modes. (a) Lower (LP), middle (MP), and upper (UP) dipolaritonic branches (solid lines), lower (LD) and upper (UD) dark exciton branches (dashed lines), uncoupled DX,IX and microcavity energies (dotted lines) versus applied voltage at zero wave vector. (b) The same branches versus wave vector at a specific voltage (4.5 V). Parameters of the branch calculations are taken to fit the results of Ref. [26].

following parameters were taken to qualitatively reproduce the results of Ref. [26]: $E_{\rm IX}(0) = 1.55$ eV, $E_{\rm DX}(0) = 1.43$ eV, $\gamma = 0.027|e|$, $\beta = 7.2 \times 10^{-16}$ eV^{-1}, $m_C = 10^{-4} m_e$, $\Omega = 6$ meV, and $J = 6$ meV. Here e and m_e stand for electron charge and mass.

Each dipolariton eigenstate is a linear combination of excitonic and photonic components with the generalized Hopfield coefficients:

$$|\mathbf{Q},S\rangle_{\rm DP} = \sum_{\rm j=IX,DX,C} c_{\rm j}(Q,V)|\mathbf{Q},S\rangle{\rm j}. \tag{2}$$

Here, the index j spans over indirect (IX), direct (DX) exciton, and cavity photon (C) states. $\mathbf{Q}$ and S designate quasimomentum and total angular momentum projection (below denoted as spin for simplicity) on the QW plane (in units of $\hbar$). These coefficients may be obtained by exact diagonalization of the Hamiltonian (1), but their analytical form is quite cumbersome and we do not present them here.

In the following sections we will be interested in the excitonic part of the dipolaritons

$$|\mathbf{Q},S\rangle_{\rm X} = c_{\rm IX}(Q,V)|\mathbf{Q},S\rangle_{\rm IX} + c_{\rm DX}(Q,V)|\mathbf{Q},S\rangle_{\rm DX}, \tag{3}$$

as it is responsible for their Coulomb interactions. The quantum states $|\mathbf{Q},S\rangle_{\rm IX}$ and $|\mathbf{Q},S\rangle_{\rm DX}$ represent an IX and a DX in the $1s$ state with center-of-mass momentum $\mathbf{Q}$ and spin $S = \pm 1$, described by wave functions having a common form with decoupled motional and spin parts [24]:

$$\Psi^{\mathbf{Q},S}(\mathbf{r}_e,\mathbf{r}_h) = \Psi^{\mathbf{Q}}(\mathbf{R})\,\Psi^{\rho}(\rho)\Psi^{z}(z_e,z_h)\chi^{S}(s_e,j_h), \tag{4}$$

where $\mathbf{R} = (m_e\mathbf{r}_e + m_h\mathbf{r}_h)_{\rm QW}/(m_e+m_h)$ is the exciton center-of-mass projection on the QW plane, $\rho = (\mathbf{r}_e - \mathbf{r}_h)_{\rm QW}$ is the in-plane distance between the electron and the hole bound into the exciton, $z_{e(h)}$ is the electron (hole) coordinate in the QW growth direction, and s_e, j_h are the electron spin and heavy hole angular momentum projections on the z axis. The center-of-mass motion part $\Psi^{\mathbf{Q}}(\mathbf{R}) = S^{-1/2}\exp(-i\mathbf{QR})$, where S is the normalization area, is the same plane wave for both types of excitons. The internal motion part $\Psi_\rho(\rho)$ reads

$$\Psi_\rho(\rho) = \frac{1}{\sqrt{2\pi b(b+r_0)}}\exp\left(\frac{-\sqrt{\rho^2+r_0^2}+r_0}{2b}\right),$$

where the b and r_0 parameters are different for IX and DX. The out-of-plane part may be set as $\Psi^z(z_e,z_h) = \delta(z_e - Z_e)\,\delta(z_h - Z_h)$, where Z_e and Z_h are the coordinates of the QWs where the electron and the hole are confined. They coincide for DX and differ in the case of IX. The spin part $\chi^S(s_e,j_h)$ plays a major role in the calculation of the scattering matrix elements, as they drastically depend on the spin configuration of a dipolariton pair. Only the exciton states with a total spin $S = \pm 1$ are coupled to the photonic mode, thus forming dipolaritons. For them we define the spin part as $\chi^{\pm 1}(s_e,j_h) = \delta_{s_e,\mp 1/2}\delta_{j_h,\pm 3/2}$.

III. POLARITON-POLARITON INTERACTIONS

In this section we shall derive the expressions for the dipolariton-dipolariton scattering matrix elements and then consider the particular case of the parametric scattering of two particles (conserving energy and momentum). We are using the perturbation theory within the Born approximation and follow the approach of Refs. [29–31] in the Sec. III A. When the corresponding contribution becomes very weak, as it happens for the interspin interaction in the range of voltages where IX and DX modes are weakly coupled, we need to proceed further to the second-order correction, which is presented in Sec. III B.

A. Born approximation

The excitonic part of a dipolariton pair state, accounting for the fermionic nature of carriers, is constructed from the direct product of two excitonic parts (3) of single dipolariton states:

$$|\mathbf{Q},S;\mathbf{Q}',S'\rangle = [|\mathbf{Q},S\rangle_{\rm X}\otimes|\mathbf{Q}',S'\rangle_{\rm X}]_a, \tag{5}$$

where the subscript a denotes the antisymmetrization with respect to the permutations of either electrons ($\mathbf{r}_e \leftrightarrow \mathbf{r}'_e$, $s_e \leftrightarrow s'_e$) or holes ($\mathbf{r}_h \leftrightarrow \mathbf{r}'_h$, $j_h \leftrightarrow j'_h$).

Considering two possible spin configurations of a scattering pair, triplet ($S = S'$), and singlet ($S = -S'$), without loss of generality we write the scattering matrix elements in the Born approximation as

$$V^{(1)}_{f\leftarrow i} = \langle f|\hat{V}|i\rangle \equiv \langle \mathbf{Q}_f,S;\mathbf{Q}'_f,S'|\hat{V}|\mathbf{Q}_i,S;\mathbf{Q}'_i,S'\rangle,$$

with $\hat{V}$ for the scattering potential, which accounts for the interexciton carrier Coulomb interactions,

$$\hat{V} = \frac{e^2}{\epsilon}\left[\frac{1}{|\mathbf{r}_e-\mathbf{r}'_e|} + \frac{1}{|\mathbf{r}_h-\mathbf{r}'_h|} - \frac{1}{|\mathbf{r}_e-\mathbf{r}'_h|} - \frac{1}{|\mathbf{r}_h-\mathbf{r}'_e|}\right],$$

where e is the electron charge and ϵ is the dielectric constant.

The matrix elements (6) may be decomposed into the following sum:

$$V^{(1)}_{f\leftarrow i} = \sum_{\rm i,j,k,l=IX,DX} C^{\rm k,l}_{\rm i,j}(Q_i,Q'_i,Q_f,Q'_f,V) \times [\langle \mathbf{Q}_f,S|_{\rm k}\otimes\langle\mathbf{Q}'_f,S'|_{\rm l}]_a\hat{V}[|\mathbf{Q}_i,S\rangle_{\rm i}\otimes|\mathbf{Q}'_i,S'\rangle_{\rm j}]_a, \tag{6}$$

where $C^{\rm k,l}_{\rm i,j} = c_{\rm i}(Q_i,V)c_{\rm j}(Q'_i,V)c^*_{\rm k}(Q_f,V)c^*_{\rm i}(Q'_f,V)$.

We consider the range of wave vectors $Q \ll a_B^{-1}$, where $a_B \sim 10$ nm is the bulk exciton Bohr radius. In this range, all quantum averages in the summation (6) are independent of the wave vectors, as their characteristic scale of variation is a_B^{-1}. Therefore the dependence on the wave vectors, as well as on the bias, is only kept in the Hopfield coefficients product $C^{\rm k,l}_{\rm i,j}(Q_i,Q'_i,Q_f,Q'_f,V)$. Finally, the vanishing overlap of DX and IX wave functions allows only the terms where either i = k, j = l or i = l, j = k to be kept and to obtain

$$V^{(1)}_{f\leftarrow i} = C^{\rm DX,DX}_{\rm DX,DX}V^{S,S'}_{\rm DX,DX} + C^{\rm IX,IX}_{\rm IX,IX}V^{S,S'}_{\rm IX,IX} + \left[C^{\rm IX,DX}_{\rm IX,DX} + C^{\rm DX,IX}_{\rm IX,DX} + C^{\rm IX,DX}_{\rm DX,IX} + C^{\rm DX,IX}_{\rm DX,IX}\right]V^{S,S'}_{\rm DX,IX}, \tag{7}$$

with interaction constants $V^{S,S'}_{\rm DX,DX}$, $V^{S,S'}_{\rm IX,IX}$, and $V^{S,S'}_{\rm DX,IX}$ representing DX-DX [11], IX-IX [23], and DX-IX [24] interactions. The corresponding matrix elements can be written as follows:

$$V^{S,S'}_{\rm i,j} = [\langle 0,S|_{\rm i}\otimes\langle 0,S'|_{\rm j}]_a\hat{V}[|0,S\rangle_{\rm i}\otimes|0,S'\rangle_{\rm j}]_a. \tag{8}$$

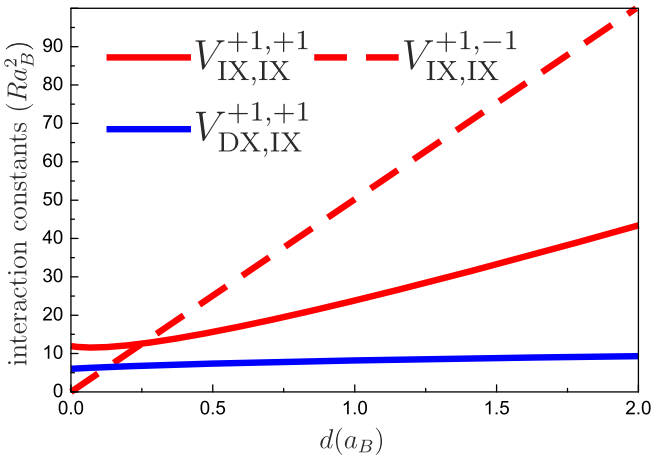

FIG. 3. (Color online) Interaction parameters calculated in Born approximation as a function of the separation distance between the QWs. The red lines represent interaction between two IXs, while the blue one corresponds to the interaction of an IX with a DX. The solid lines describe the interaction of two excitons with the same spin (α_1^{II},α_1^{DI}) and the dashed one is for two excitons with opposite spins (α_2^{II}).

where i,j span over IX,DX. The spin dependence of each of the above integrals is then conveniently described by its decomposition into a sum of four terms with evident spin parts:

$$V_{\mathrm{i,j}}^{S,S'} = V_{\mathrm{i,j}}^{\mathrm{dir}} + \delta_{S,S'} V_{\mathrm{i,j}}^{\mathrm{X}} + \delta_{s_e,s_e'} V_{\mathrm{i,j}}^{\mathrm{e}} + \delta_{j_h,j_h'} V_{\mathrm{i,j}}^{\mathrm{h}}. \tag{9}$$

The first term represents the direct dipole-dipole interaction and is present for any combination of exciton spins. The second term describes the exciton exchange contribution and accounts for the bosonic nature of the exciton. Finally, the last two terms represent the electron and hole exchange contributions, accounting for the fermionic nature of the carriers. Matrix elements (8) are evidently expressed in these terms:

$$\begin{aligned} V_{\mathrm{i,j}}^{+1,+1} &= V_{\mathrm{i,j}}^{\mathrm{dir}} + V_{\mathrm{i,j}}^{\mathrm{X}} + V_{\mathrm{i,j}}^{\mathrm{e}} + V_{\mathrm{i,j}}^{\mathrm{h}}, \\ V_{\mathrm{ij}}^{+1,-1} &= V_{\mathrm{i,j}}^{\mathrm{dir}}. \end{aligned} \tag{10}$$

Neglecting the DX dipole with respect to that of the IX results in $V_{\mathrm{DX,DX}}^{+1,-1} = V_{\mathrm{DX,IX}}^{+1,-1} = 0$. Figure 3 shows the dependence of nonzero matrix elements (10) on the QW separation distance d. The zero separation limit corresponds to the transition from IX to DX. At $d \approx a_B/4$, the carrier exchange contribution changes sign and therefore $V_{\mathrm{IX,IX}}^{+1,-1} > V_{\mathrm{IX,IX}}^{+1,+1}$ for $d > a_B/4$.

Note that $V_{\mathrm{DX,IX}}^{+1,+1}$, plotted by the blue line, is inaccurate in the vicinity of point $d = 0$, where the IX and DX are indistinguishable. Moreover, the range where the distance between the QW centers is shorter than their widths is physically meaningless.

Setting $i = f = |\mathbf{Q},S,\mathbf{Q},S'\rangle$ states that at a given point of the energy dispersion branches, we calculate the effective dipolaritonic interaction constants α_1 and α_2 responsible for frequency shifting of dipolaritonic luminescence due to interaction between dipolaritons with the same (α_1) and

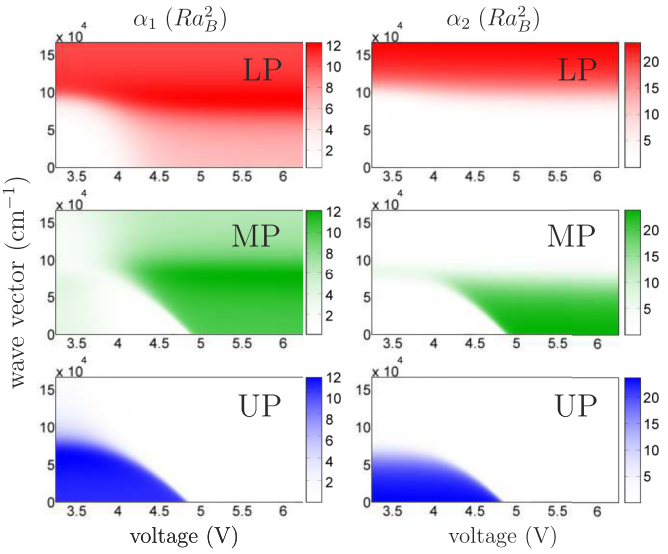

FIG. 4. (Color online) Interaction constants responsible for the blueshift and the bistability of pumped dipolariton states calculated in the Born approximation. Left and right columns correspond to α_1 and α_2, while the three rows correspond to LP, MP, and UP dipolariton branches. The voltage and wave-vector dependencies are due to the variation of Hopfield coefficients.

opposite (α_2) spins, as quantum averages (6):

$$\begin{aligned} \alpha_1 &= |c_{\mathrm{DX}}(Q,V)|^4 V_{\mathrm{DX,DX}}^{+1,+1} + |c_{\mathrm{IX}}(Q,V)|^4 V_{\mathrm{IX,IX}}^{+1,+1} \\ &\quad + 4|c_{\mathrm{DX}}(Q,V)|^2 |c_{\mathrm{IX}}(Q,V)|^2 V_{\mathrm{DX,IX}}^{+1,+1}, \\ \alpha_2 &= |c_{\mathrm{IX}}(Q,V)|^4 V_{\mathrm{IX,IX}}^{+1,-1}. \end{aligned} \tag{11}$$

Figure 4 presents the results of the numerical calculation of these constants throughout the three dipolaritonic branches in dependence on the applied bias. Note that $\alpha_{1(2)}$ reflects a blueshift of photoluminescence in a particular circular polarization due to optical pumping with the same (opposite) circular polarization.

All listed interaction constants are positive; therefore the dipolariton scattering matrix elements (8) obtained in this section describe only repulsive interactions. In order to include the dipolariton attraction in our model, we continue the expansion of the interactions to the second order.

B. Second-order corrections

In this section, we study the second-order corrections to the interaction matrix elements, which are important for a scattering of two dipolaritons with opposite spins in the region of voltages and momenta where the IX fraction of either the initial or final state is small and so is the first-order matrix element. This condition can be satisfied for the voltages where $|E_{\mathrm{I}} - E_{\mathrm{D}}| \gg J$. One can expect the change of sign of the singlet interaction parameter α_2 at the point where the first- and the second-order contributions become comparable.

Scattering of two polaritons with opposite spins has been recently studied theoretically [12] and experimentally [13]. In particular, Ref. [13] reports a strong attraction of singlet lower-branch polariton pairs depending on the energy detuning between the DX and cavity modes.

We start to generalize the results of Ref. [12] to the case of lower-branch dipolaritons with the expression for the correction to the scattering matrix element in the second order of the perturbation theory [32]:

$$V_{f\leftarrow i}^{(2)\uparrow\downarrow} = \sum_m \frac{\langle f|\hat{V}|m\rangle\langle m|\hat{V}|i\rangle}{E_i - E_m} \equiv \sum_m \frac{\langle \mathbf{Q}_f, +1; \mathbf{Q}'_f, -1|\hat{V}|m\rangle\langle m|\hat{V}|\mathbf{Q}_i, +1; \mathbf{Q}'_i, -1\rangle}{E_i - E_m}, \tag{12}$$

where m enumerates all intermediate states of two electrons and two holes playing the role of the interaction mediator.

Intermediate states representing two dipolaritons with opposite spins are coupled with initial and final states by spin conserving dipole-dipole scattering and result in a second-order correction to the repulsion. On the contrary, states formed by two "dark" excitons $|\mathbf{Q}+\mathbf{P}, +2; \mathbf{Q}'-\mathbf{P}, -2\rangle$ are coupled to dipolariton pair states $|\mathbf{Q}, +1; \mathbf{Q}', -1\rangle$ via virtual fermion exchange. Terms with such intermediate states give a negative contribution to the interaction potential exceeding the first-order repulsion in absolute value. The same applies to the contribution coming from biexcitonic intermediate states. It becomes important in the case of polaritonic Feshbach resonance [14], when the dipolariton pair energy coincides with the biexciton energy and expression (12) diverges. In this work, we consider polariton states being far from the biexciton and dark exciton resonance, so that both terms give qualitatively the same type of contributions. Then, in order to simplify the calculations, we neglect the biexciton states' contribution and focus on the contribution of dark exciton states.

Due to the electron tunneling through the barrier, the dark IX and DX states are coupled and form two anticrossing branches LD and UD, plotted with dashed lines in Fig. 2. Direct and indirect fractions $d_{\mathrm{D}}^{\mathrm{LD(UD)}}$ and $d_{\mathrm{I}}^{\mathrm{LD(UD)}}$ of the dark branches, obtained by diagonalization of the Hamiltonian (1) with $\Omega = 0$, are independent of Q due to equal IX and DX effective masses. Similar to the previous section, we derive the following:

$$V_{f\leftarrow i}^{(2)\uparrow\downarrow} = \sum_{\mathrm{i,j,k,l=IX,DX}}^{\mathrm{m,n=LD,UD}} C_{\mathrm{i,j}}^{\mathrm{k,l}} D_{\mathrm{i,j,k,l}}^{\mathrm{m,n}} \times \sum_{\mathbf{P}} \frac{V_{\mathrm{k,l}}^{\mathrm{exch}}(P) V_{\mathrm{i,j}}^{\mathrm{exch}}(P)}{-\Delta_{\mathrm{m,n}} - \hbar^2 P^2/M_X},$$

where $D_{\mathrm{i,j,k,l}}^{\mathrm{m,n}}(V) = d_{\mathrm{i}}^{\mathrm{m}}(V) d_{\mathrm{j}}^{\mathrm{n}}(V) d_{\mathrm{k}}^{\mathrm{m}}(V) d_{\mathrm{l}}^{\mathrm{n}}(V)$ and $\Delta_{\mathrm{m,n}}(V) = E_{\mathrm{m}}(V) + E_{\mathrm{n}}(V) - E_i$. Here, we neglect once again the dependence of the virtual fermion exchange matrix elements $V_{\mathrm{i,j}}^{\mathrm{exch}}(P)$ on the dipolariton momenta $Q \ll a_B$, although we keep the virtual transferred momentum $\mathbf{P}$ which spans over the whole reciprocal space. Furthermore, we omit the terms where $\mathrm{i} = \mathrm{j} = \mathrm{IX}$ and $\mathrm{k} = \mathrm{l} = \mathrm{IX}$, representing the next-order correction to the IX repulsive contribution. The virtual exchange matrix elements are

$$V_{\mathrm{IX,DX}}^{\mathrm{exch}}(P) = [\langle 0,+1|_{\mathrm{IX}} \otimes \langle 0,-1|_{\mathrm{DX}}]_a \hat{V} [|\mathbf{P}, -2\rangle_{\mathrm{IX}} \otimes |-\mathbf{P},+2\rangle_{\mathrm{DX}}]_a,$$

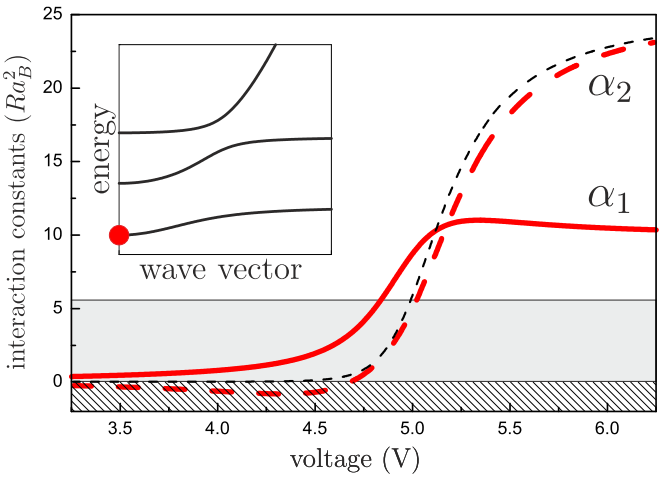

FIG. 5. (Color online) Effective interaction parameters responsible for blueshift, bistability, and polarization of the ground dipolariton state (sketched in the inset), calculated in the second order of the perturbation theory, are plotted in red. Interaction parameter α_2, describing the interaction potential of two dipolaritons with opposite spins, changes sign with voltage and even exceeds α_1, the one describing two dipolaritons with aligned spins. The gray(hatched) area represents possible values of α_1 (α_2) for conventional polaritons. The result of the first-order calculation of α_2 is plotted with a black dashed line for comparison.

$$V_{\mathrm{DX,DX}}^{\mathrm{exch}}(P) = [\langle 0,+1|_{\mathrm{DX}} \otimes \langle 0,-1|_{\mathrm{DX}}]_a \hat{V} [|\mathbf{P},-2\rangle_{\mathrm{DX}} \otimes |-\mathbf{P},+2\rangle_{\mathrm{DX}}]_a + [\langle 0,+1|_{\mathrm{DX}} \otimes \langle 0,-1|_{\mathrm{DX}}]_a \hat{V} [|\mathbf{P},+2\rangle_{\mathrm{DX}} \otimes |-\mathbf{P},-2\rangle_{\mathrm{DX}}]_a.$$

Note that the two terms of the latter correspond to electron and hole exchange, contrary to the IX-DX case, where only the hole exchange is possible. Both matrix elements are integrated numerically in dependence on the transferred momentum [11,24] and vanish at $P > a_B/2$.

Substituting the two-particle ground dipolariton state as both i and f into Eqs. (7) and (12), we calculate the effective interaction constants for the ground state. The results of this calculation are plotted in Fig. 5. One can observe that α_2 is changing sign at some particular voltage, similar to the case of resonant interaction with the biexciton resonance [13,14], which has the disadvantage of inducing strong losses. Here, the mechanism is the increase of the mixing with the IX state, which does not add any losses to the dipolariton. However, the whole system can be possibly affected by the large intrinsic losses of the dipolaritonic states, induced by the presence of the metallic contacts and doped mirrors. A second remarkable point occurs at a slightly larger voltage, when α_2 and α_1 become equal. In the case of a dipolariton condensation, this boundary corresponds to a transition between linearly and circularly polarized states [13] which can therefore be tuned, simply by changing the applied voltage.

IV. OPTICAL PARAMETRIC OSCILLATOR

The OPO configuration of the dipolariton excitation scheme implies parametric scattering of two quasiparticles from the

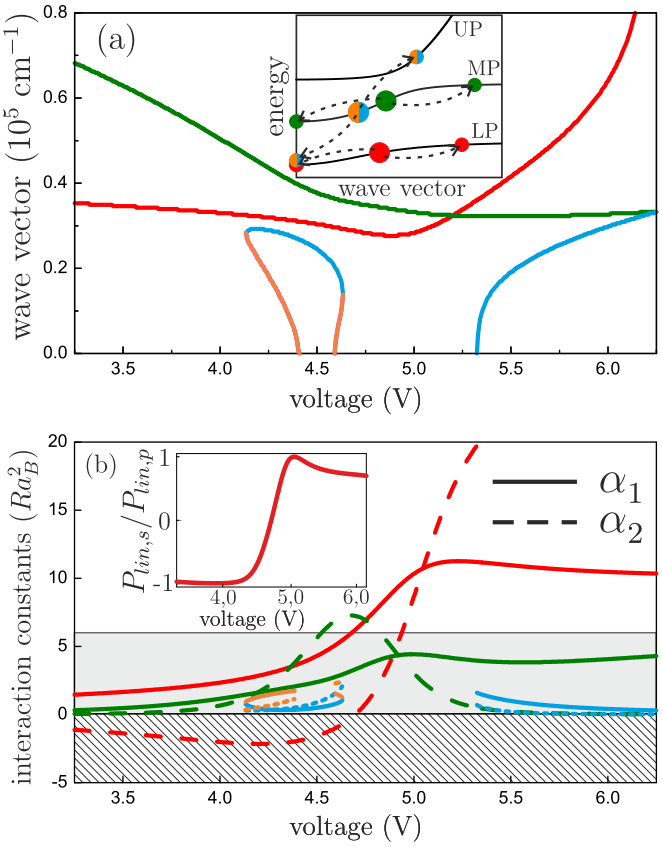

FIG. 6. (Color online) Optical parametric oscillator properties. (a) Numerical solution of energy-momentum conservation law for parametric scattering, sketched on the inset. Two dipolaritons in the pump state (large circles) scatter to signal and idler states (small circles). Depending on applied bias there are from 2 to 4 solutions corresponding to different scattering configurations. The wave vector of the pump state, representing the magic angle of optical excitation, is plotted with colors corresponding to the following configurations: red and green for scattering within LP and MP branches, orange and magenta for interbranch scattering. (b) Interaction constants calculated for dipolariton parametric scattering in the second order of the perturbation theory. Solid lines represent interaction between the dipolaritons with the same spin (α_1), dashed lines are for dipolaritons with opposite spins (α_2). The gray (hatched) area limits the possible values of α_1 (α_2) for conventional microcavity polaritons. Both LP and MP configurations have a range of voltages where $\alpha_2 > \alpha_1$. In the LP case, α_2 is changing sign due to variation of the energy detuning and dipolariton oscillator strength. The inset shows the relation between linear polarization degrees of signal emission and optical pumping in the most relevant case of LP parametric scattering.

resonantly excited pump state (Q_p), conserving the energy and the momentum into the signal ($Q_s = 0$) and idler (Q_i) states, schematically shown in the inset of Fig. 6(a). The numerical solution of in-plane momentum and energy conservation equations,

$$2Q_p = Q_s + Q_i, \quad 2E_p = E_s + E_i, \tag{13}$$

gives all possible pump state wave vectors, satisfying the OPO condition, as a function of the applied voltage, plotted in Fig. 6(a). Note that in contrast with the single-branch OPO schemes, where all states involved in the OPO lie on the same branch (for example, lower polariton branch), the ASDQW structure permits in principle an interbranch OPO scheme with LP signal, MP pump, and UP idler states. Such an OPO configuration may be used for generation of entangled photon pairs as both signal and idler states are photonic; therefore the problem of idler polariton coherence loss due to the strong excitonic interactions is avoided. The UP branch alone does not provide a possibility of a single-branch OPO scheme due to the absence of an inflection point. Moreover, the states lying above the bare exciton energy are resonantly coupled to a large density of excitonic states and can suffer from a significant dephasing, even if their excitonic fraction is small. This dephasing is not accounted for in our approach. The resonant pumping of the LP is therefore the only configuration which we expect to be properly described by our approach.

The spin kinetics of the system strongly depend on the type of polariton-polariton interaction. Polarization of photons, emitted from the signal state once the OPO turns on, is defined by polarization of pumping and two interaction constants α_1 and α_2 describing parametric scattering of a pair of dipolaritons with aligned and antialigned spins, respectively. In the particular case of linearly polarized pumping, the signal linear polarization degree is expressed by a simple relation [20]

$$P_{lin,s} = \frac{\alpha_1\alpha_2}{\alpha_1^2 + \alpha_2^2} P_{lin,p}, \tag{14}$$

where $P_{lin,p}$ is the linear polarization of the optical pumping. The sign of $P_{lin,s}$ and thus the orientation of the signal polarization plane, are therefore determined by the relative sign of the interaction parameters α_1 and α_2 describing parametric scattering of dipolaritons with aligned and opposite spins.

To calculate them accounting for the second-order correction, we substitute the pump, signal, and idler dipolariton states into Eqs. (7) and (12):

$$\begin{aligned}
\alpha_1 = {} & c_{\mathrm{DX}}^2(Q_p,V)c_{\mathrm{DX}}(Q_s,V)^*c_{\mathrm{D}}(Q_i,V)^*V_{\mathrm{DX,DX}}^{+1,+1} \\
& + c_{\mathrm{IX}}^2(Q_p,V)c_{\mathrm{IX}}(Q_s,V)^*c_{\mathrm{IX}}(Q_i,V)^*V_{\mathrm{IX,IX}}^{+1,+1} \\
& + 2c_{\mathrm{IX}}(Q_p,V)c_{\mathrm{DX}}(Q_p,V))[c_{\mathrm{DX}}(Q_s,V)^*c_{\mathrm{IX}}(Q_i,V)^* \\
& + c_{\mathrm{DX}}(Q_s,V)^*c_{\mathrm{IX}}(Q_i,V)^*]V_{\mathrm{DX,IX}}^{+1,+1}, \\
\alpha_2 = {} & c_{\mathrm{IX}}^2(Q_p,V)c_{\mathrm{IX}}(Q_s,V)^*c_{\mathrm{IX}}(Q_i,V)^*V_{\mathrm{IX,IX}}^{+1,-1} \\
& + \sum_{\mathrm{i,j,k,l=IX,DX}}^{\mathrm{m,n=LD,UD}} c_{\mathrm{i}}(Q_p,V)c_{\mathrm{j}}(Q_p,V)c_{\mathrm{k}}(Q_s,V)^*c_{\mathrm{l}}(C_i,V)^* \\
& \times d_{\mathrm{i}}^{\mathrm{m}}(V)d_{\mathrm{j}}^{\mathrm{n}}(V)d_{\mathrm{k}}^{\mathrm{m}}(V)d_{\mathrm{l}}^{\mathrm{n}}(V)\sum_{\mathbf{P}} \frac{V_{\mathrm{k,l}}^{\mathrm{exch}}(P)V_{\mathrm{i,j}}^{\mathrm{exch}}(P)}{-\Delta_{\mathrm{m,n}} - \hbar^2P^2/M_X}.
\end{aligned} \tag{15}$$

The results of this calculation are plotted in Fig. 5(b) for LP, MP, and interbranch scattering configurations. Notably, the following situations may be achieved by voltage variation for different OPO configurations: (i) $\alpha_2 < 0$, linear polarization inversion is on; (ii) $0 < \alpha_2 < \alpha_1$, and (iii) $\alpha_2 > \alpha_1$, linear polarization inversion is off. Moreover, as can be seen in Fig. 5(b), in a certain range of voltages, the dipolaritonic OPO interaction constant exceeds the theoretically achievable value of $\alpha_1 = 6Ra_B^2$ for conventional microcavity polaritons [12].

Substitution of the calculated interaction constants into relation (14) finally gives the dependence of the signal linear polarization degree on the applied bias for the case of full linear polarization of the pumping ($P_{lin,p} = 1$), plotted in the inset of Fig. 5(b). It has a fast switching region from negative to positive values in the vicinity of the crossing point of the three modes, where α_2 value crosses zero. Realistically, the absolute value of the signal polarization degree is lowered by spin relaxation processes. However, the main result is that the orientation of the signal emission polarization plane may be switched between that of the optical pump and the one orthogonal to it.

V. CONCLUSION

We have calculated the spin-dependent interaction parameters for dipolaritons and analyzed the specific role played by the dipolar interaction between indirect excitons. We have shown that these parameters can be 1 order of magnitude larger than for conventional polaritons. By tuning the applied voltage, the interaction parameter α_2 between dipolaritons with opposite spin changes sign and can become larger than α_1—the interaction parameter between dipolaritons having the same spin.

This shows that dipolaritons are promising particles for spin-optronic applications. In particular, we consider a dipolaritonic OPO scheme, which, due to the large values of the interaction parameters, has a very low threshold. It offers the possibilities of interbranch parametric scattering. Flipping the sign of the singlet interaction α_2 parameter allows the on-demand linear polarization inversion switching and polarization degree control by the applied bias.

ACKNOWLEDGMENTS

This work has been supported by EU FP7 ITN INDEX (Contract No. 289968) and ANR QUANDYDE (Contract No. ANR-11-BS10-001). N.G. acknowledges support from the RFBR and the Ministry of Education and Science of Russian Federation (Project No. RFMEFI58114X0006). We thank M. Glazov for fruitful discussions.

[1] A. V. Kavokin, J. J. Baumberg, G. Malpuech, and F. P. Laussy, *Microcavities*, edited by R. J. Nicholas and H. Kamimura (Oxford University Press, Oxford, UK, 2007).
[2] I. Carusotto and C. Ciuti, Rev. Mod. Phys. **85**, 299 (2013).
[3] P. G. Savvidis, J. J. Baumberg, R. M. Stevenson, M. S. Skolnick, D. M. Whittaker, and J. S. Roberts, Phys. Rev. Lett. **84**, 1547 (2000).
[4] G. Messin, J. P. Karr, A. Baas, G. Khitrova, R. Houdré, R. P. Stanley, U. Oesterle, and E. Giacobino, Phys. Rev. Lett. **87**, 127403 (2001).
[5] T. Paraiso, M. Wouters, Y. Leger, F. Mourier-Genoud, and B. Deveaud-Pledran, Nature Mater. **9**, 655 (2010).
[6] T. Gao, P. S. Eldridge, T. C. H. Liew, S. I. Tsintzos, G. Stavrinidis, G. Deligeorgis, Z. Hatzopoulos, and P. G. Savvidis, Phys. Rev. B **85**, 235102 (2012).
[7] H. S. Nguyen, D. Vishnevsky, C. Sturm, D. Tanese, D. Solnyshkov, E. Galopin, A. Lemaitre, I. Sagnes, A. Amo, G. Malpuech, and J. Bloch, Phys. Rev. Lett. **110**, 236601 (2013).
[8] C. Sturm, D. Tanese, H. Nguyen, H. Flayac, E. Galopin, A. Lemaître, I. Sagnes, D. D. Solnyshkov, D. Amo, G. Malpuech, and J. Bloch, Nat. Commun. **5**, 3278 (2014).
[9] F. Li, L. Orosz, O. Kamoun, S. Bouchoule, C. Brimont, P. Disseix, T. Guillet, X. Lafosse, M. Leroux, J. Leymarie, M. Mexis, M. Mihailovic, G. Patriarche, F. Réveret, D. Solnyshkov, J. Zuniga-Perez, and G. Malpuech, Phys. Rev. Lett. **110**, 196406 (2013).
[10] I. A. Shelykh, A. V. Kavokin, Y. G. Rubo, T. C. H. Liew, and G. Malpuech, Semicond. Sci. Technol. **25**, 013001 (2010).
[11] C. Ciuti, V. Savona, C. Piermarocchi, A. Quattropani, and P. Schwendimann, Phys. Rev. B **58**, 7926 (1998).
[12] M. M. Glazov, H. Ouerdane, L. Pilozzi, G. Malpuech, A. V. Kavokin, and A. D'Andrea, Phys. Rev. B **80**, 155306 (2009).
[13] M. Vladimirova, S. Cronenberger, D. Scalbert, K. V. Kavokin, A. Miard, A. Lemaître, J. Bloch, D. Solnyshkov, G. Malpuech, and A. V. Kavokin, Phys. Rev. B **82**, 075301 (2010).
[14] N. Takemura, S. Trebaol, M. Wouters, M. T. Portella-Oberli, and B. Deveaud, Nat. Phys. **10**, 500 (2014).
[15] I. A. Shelykh, Y. G. Rubo, G. Malpuech, D. D. Solnyshkov, and A. Kavokin, Phys. Rev. Lett. **97**, 066402 (2006).
[16] J. Kasprzak, M. Richard, S. Kundermann, A. Baas, P. Jeambrun, J. M. J. Keeling, F. M. Marchetti, M. H. Szymanska, R. Andre, J. L. Staehli, V. Savona, P. B. Littlewood, B. Deveaud, and L. S. Dang, Nature (London) **443**, 409 (2006).
[17] J. Kasprzak, R. André, L. S. Dang, I. A. Shelykh, A. V. Kavokin, Y. G. Rubo, K. V. Kavokin, and G. Malpuech, Phys. Rev. B **75**, 045326 (2007).
[18] Y. G. Rubo, Phys. Rev. Lett. **99**, 106401 (2007).
[19] D. D. Solnyshkov, H. Flayac, and G. Malpuech, Phys. Rev. B **85**, 073105 (2012).
[20] P. Renucci, T. Amand, X. Marie, P. Senellart, J. Bloch, B. Sermage, and K. V. Kavokin, Phys. Rev. B **72**, 075317 (2005).
[21] N. A. Gippius, I. A. Shelykh, D. D. Solnyshkov, S. S. Gavrilov, Y. G. Rubo, A. V. Kavokin, S. G. Tikhodeev, and G. Malpuech, Phys. Rev. Lett. **98**, 236401 (2007).
[22] D. V. Vishnevsky, D. D. Solnyshkov, N. A. Gippius, and G. Malpuech, Phys. Rev. B **85**, 155328 (2012).
[23] O. Kyriienko, E. B. Magnusson, and I. A. Shelykh, Phys. Rev. B **86**, 115324 (2012).
[24] A. V. Nalitov, M. Vladimirova, A. V. Kavokin, L. V. Butov, and N. A. Gippius, Phys. Rev. B **89**, 155309 (2014).
[25] P. Cristofolini, G. Christmann, S. I. Tsintzos, G. Deligeorgis, G. Konstantinidis, Z. Hatzopoulos, P. G. Savvidis, and J. J. Baumberg, Science **336**, 704 (2012).
[26] C. Coulson, G. Christmann, P. Cristofolini, C. Grossmann, J. J. Baumberg, S. I. Tsintzos, G. Konstantinidis, Z. Hatzopoulos, and P. G. Savvidis, Phys. Rev. B **87**, 045311 (2013).
[27] D. A. B. Miller, D. S. Chemla, T. C. Damen, A. C. Gossard, W. Wiegmann, T. H. Wood, and C. A. Burrus, Phys. Rev. Lett. **53**, 2173 (1984).

[28] K. Sivalertporn, L. Mouchliadis, A. L. Ivanov, R. Philp, and E. A. Muljarov, Phys. Rev. B **85**, 045207 (2012).
[29] E. Hanamura and H. Haug, Phys. Rep. **33**, 209 (1977).
[30] G. Rochat, C. Ciuti, V. Savona, C. Piermarocchi, A. Quattropani, and P. Schwendimann, Phys. Rev. B **61**, 13856 (2000).
[31] C. Ciuti, P. Schwendimann, and A. Quattropani, Semicond. Sci. Technol. **18**, S279 (2003).
[32] L. D. Landau and E. M. Lifshitz, *Quantum Mechanics: NonRelativistic Theory*, Vol. 3 (Butterworth-Heinemann, Oxford, UK, 1977).